



Universiteit  
Leiden  
The Netherlands

## **Beneficial effects of chronic mexiletine treatment in a human model of SCN5A overlap syndrome**

Nasilli, G.; Yiangou, L.; Palandri, C.; Cerbai, E.; Davis, R.P.; Verkerk, A.O.; ... ; Remme, C.A.

### **Citation**

Nasilli, G., Yiangou, L., Palandri, C., Cerbai, E., Davis, R. P., Verkerk, A. O., ... Remme, C. A. (2023). Beneficial effects of chronic mexiletine treatment in a human model of SCN5A overlap syndrome. *Ep Europace*, 25(6). doi:10.1093/europace/euad154

Version: Publisher's Version

License: [Creative Commons CC BY-NC 4.0 license](https://creativecommons.org/licenses/by-nc/4.0/)

Downloaded from: <https://hdl.handle.net/1887/3750147>

**Note:** To cite this publication please use the final published version (if applicable).

# Beneficial effects of chronic mexiletine treatment in a human model of SCN5A overlap syndrome

Giovanna Nasilli <sup>1,2</sup>, Loukia Yiangou <sup>3</sup>, Chiara Palandri <sup>4</sup>,  
 Elisabetta Cerbai <sup>4</sup>, Richard P. Davis <sup>3,5</sup>, Arie O. Verkerk <sup>1,2,6</sup>,  
 Simona Casini <sup>1,2,\*†</sup>, and Carol Ann Remme <sup>1,2,\*†</sup>

<sup>1</sup>Department of Experimental Cardiology, Amsterdam University Medical Center, University of Amsterdam, Heart Centre, Meibergdreef 9, 1105 AZ, Amsterdam, The Netherlands; <sup>2</sup>Amsterdam Cardiovascular Sciences, Heart Failure & Arrhythmias, Amsterdam, The Netherlands; <sup>3</sup>Department of Anatomy and Embryology, Leiden University Medical Center, Albinusdreef 2, 2300 RC, Leiden, The Netherlands; <sup>4</sup>Department NeuroFarBa, University of Florence, Viale Gaetano Pieraccini 6, 50139, Florence, Italy; <sup>5</sup>The Novo Nordisk Foundation Center for Stem Cell Medicine (reNEV), Albinusdreef 2, 2300 RC, Leiden, The Netherlands; and <sup>6</sup>Department of Medical Biology, Amsterdam University Medical Center, University of Amsterdam, Meibergdreef 9, 1105 AZ, Amsterdam, The Netherlands

Received 20 March 2023; accepted after revision 31 May 2023

## Aims

SCN5A mutations are associated with various cardiac phenotypes, including long QT syndrome type 3 (LQT3), Brugada syndrome (BrS), and cardiac conduction disease (CCD). Certain mutations, such as SCN5A-1795insD, lead to an overlap syndrome, with patients exhibiting both features of BrS/CCD [decreased sodium current ( $I_{Na}$ )] and LQT3 (increased late  $I_{Na}$ ). The sodium channel blocker mexiletine may acutely decrease LQT3-associated late  $I_{Na}$  and chronically increase peak  $I_{Na}$  associated with SCN5A loss-of-function mutations. However, most studies have so far employed heterologous expression systems and high mexiletine concentrations. We here investigated the effects of a therapeutic dose of mexiletine on the mixed phenotype associated with the SCN5A-1795insD mutation in HEK293A cells and human-induced pluripotent stem cell-derived cardiomyocytes (hiPSC-CMs).

## Methods and results

To assess only the chronic effects on trafficking, HEK293A cells transfected with wild-type (WT) SCN5A or SCN5A-1795insD were incubated for 48 h with 10  $\mu$ M mexiletine followed by wash-out, which resulted in an increased peak  $I_{Na}$  for both SCN5A-WT and SCN5A-1795insD and an increased late  $I_{Na}$  for SCN5A-1795insD. Acute re-exposure of HEK293A cells to 10  $\mu$ M mexiletine did not impact on peak  $I_{Na}$  but significantly decreased SCN5A-1795insD late  $I_{Na}$ . Chronic incubation of SCN5A-1795insD hiPSC-CMs with mexiletine followed by wash-out increased peak  $I_{Na}$ , action potential (AP) upstroke velocity, and AP duration. Acute re-exposure did not impact on peak  $I_{Na}$  or AP upstroke velocity, but significantly decreased AP duration.

## Conclusion

These findings demonstrate for the first time the therapeutic benefit of mexiletine in a human cardiomyocyte model of SCN5A overlap syndrome.

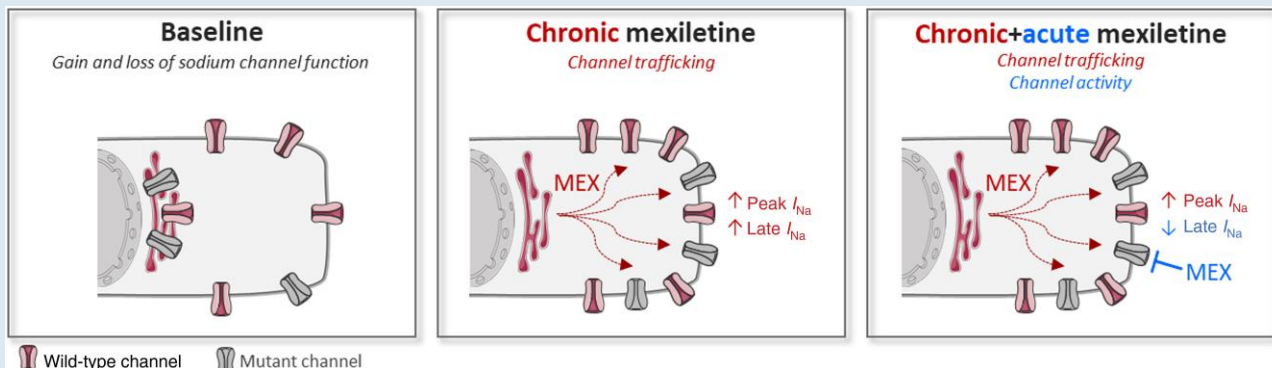
\* Corresponding authors. Tel: +31 20 5663262, E-mail address: c.a.remme@amsterdamumc.nl (C.A.R.); Tel: +31 20 5668544, E-mail address: s.casini@amsterdamumc.nl (S.C.)

† The last two authors contributed equally to the study.

© The Author(s) 2023. Published by Oxford University Press on behalf of the European Society of Cardiology.

This is an Open Access article distributed under the terms of the Creative Commons Attribution-NonCommercial License (<https://creativecommons.org/licenses/by-nc/4.0/>), which permits non-commercial re-use, distribution, and reproduction in any medium, provided the original work is properly cited. For commercial re-use, please contact journals.permissions@oup.com

## Graphical Abstract



$I_{Na}$ , sodium current.

## Keywords

Ion channels • Cardiac electrophysiology • *SCN5A* • Sudden cardiac death • Therapy

## What's new?

- Mexiletine may acutely inhibit late sodium current and chronically enhance sodium channel trafficking through its 'chaperone' effect and hence may be beneficial in *SCN5A* overlap syndromes.
- We here show that the latter can already be achieved by chronic treatment with a clinically relevant concentration of mexiletine.
- We identify mexiletine as a novel approach to rescue decreased peak sodium current, which may prove beneficial in other inherited arrhythmia disorders.
- We furthermore demonstrate for the first time the therapeutic benefit of mexiletine in a human cardiomyocyte model of *SCN5A* overlap syndrome.

## Introduction

The cardiac sodium channel  $Na_v1.5$  is essential for excitability and electrical conduction in the heart.  $Na_v1.5$  is encoded by the *SCN5A* gene and is located on the membrane of cardiomyocytes (CMs), where it allows the influx of sodium ions leading to the rapid upstroke of the action potential (AP).<sup>1</sup> Mutations in *SCN5A* cause biophysical changes in sodium current ( $I_{Na}$ ), which can lead to different cardiac disorders with distinct clinical features.<sup>2,3</sup> Gain-of-function *SCN5A* mutations responsible for the long QT syndrome type 3 (LQT3) typically lead to an increased late  $I_{Na}$ , while loss-of-function *SCN5A* mutations associated with conduction disease and Brugada syndrome (BrS) cause a decrease in peak  $I_{Na}$ .<sup>4</sup> In some instances, a single *SCN5A* mutation can lead to a double phenotype, showing characteristics of both gain- and loss-of-function, as is the case for the *SCN5A*-1795insD mutation.<sup>5–7</sup> This mutation causes an 'overlap syndrome', with affected individuals displaying electrocardiogram (ECG) characteristics of cardiac conduction disorder, BrS, and LQT3, in addition to a high risk for (nocturnal) sudden death. Accordingly, the mutation leads to both a reduced peak  $I_{Na}$  and an increased late  $I_{Na}$ .<sup>5–7</sup>

Pharmacological therapeutic options for patients carrying *SCN5A* mutations are limited.  $\beta$ -Blockers are often prescribed in LQT3 but they do not show benefit in all patients.<sup>8,9</sup> Moreover, the management of individuals with an overlap syndrome may be even more complicated. Pacemaker therapy, aimed at preventing (nocturnal) bradycardia-dependent QT prolongation, was initially considered efficacious in

*SCN5A*-1795insD patients; however, a subset of patients experienced ventricular arrhythmias despite pacemaker therapy,<sup>10</sup> indicating a need for additional therapeutic approaches. Mexiletine, a Class Ib antiarrhythmic drug and sodium channel blocker, may shorten QT interval by inhibiting late  $I_{Na}$  in LQT3 patients and has shown benefits in patients with structural heart disease and at risk of recurrent ventricular arrhythmia,<sup>11,12</sup> although its beneficial effects are mutation-dependent.<sup>13</sup> In addition, incubation with mexiletine for 24–48 h has been shown to rescue the reduced peak  $I_{Na}$  associated with certain loss-of-function *SCN5A* mutations, most likely by restoring membrane trafficking of  $Na_v1.5$  channels.<sup>14–18</sup> However, the majority of these studies used very high, non-therapeutic concentrations (>100  $\mu$ M) of mexiletine. Moreover, the investigations were performed in heterologous expression systems (such as HEK293A cells), which, although informative, do not fully recapitulate the cardiomyocyte environment.

Nevertheless, given the potential beneficial effects of mexiletine on both gain (increased late  $I_{Na}$ ) and loss (decreased peak  $I_{Na}$ ) of function mutations, we here hypothesized that it could ameliorate the overlap syndrome phenotype associated with the *SCN5A*-1795insD mutation. Using HEK293A cells, we show that chronic administration of a therapeutic concentration of 10  $\mu$ M (clinical range 2.8–11  $\mu$ M)<sup>19–21</sup> mexiletine increases both wild-type (WT) and *SCN5A*-1795insD peak  $I_{Na}$ , while it acutely decreased the mutation-associated late  $I_{Na}$ . Importantly, chronic mexiletine therapy increased peak  $I_{Na}$  and AP upstroke velocity in human-induced pluripotent stem cell-derived cardiomyocytes (hiPSC-CMs) carrying the *SCN5A*-1795insD mutation, while its acute administration decreased AP duration (APD). These findings demonstrate for the first time the therapeutic benefit of mexiletine in a human cardiomyocyte model of *SCN5A* overlap syndrome.

## Methods

### Site-directed mutagenesis

Site-directed mutagenesis was performed on *SCN5A*-WT cDNA cloned in pSP64T, as previously described.<sup>5</sup> *SCN5A*-1795insD cDNA was then subcloned into the *HindIII*–*XbaI* sites of the expression vector pCGI for bicistronic expression of the channel protein and GFP reporter in HEK293A cells.

### Transfection of HEK293A cells

HEK293A cells were cultured with DMEM medium (Dulbecco's modified Eagle's medium 21969-035 from Thermo Fisher Scientific) supplemented with 10% foetal bovine serum, 1% L-glutamine (Thermo Fisher Scientific),

and 1% penicillin–streptomycin (Thermo Fisher Scientific) in a 5% CO<sub>2</sub> incubator at 37°C. At ~70% confluency, HEK293A cells were transfected with 0.2 µg of cardiac sodium channel  $\alpha$ -subunit cDNA (only SCN5A-WT or only SCN5A-1795insD) and 0.2 µg human  $\beta_1$ -subunit cDNA using Lipofectamine 3000 (Thermo Fisher Scientific).

## Generation of human-induced pluripotent stem cell-derived cardiomyocytes

SCN5A-1795insD hiPSC were differentiated into CMs, cryopreserved and thawed as previously described.<sup>22</sup> In summary, glass coverslips were coated with 1:100 matrigel in DMEM-F12 (Thermo Fisher Scientific) for 2 h at 37°C before thawed hiPSC-CMs were seeded at a density of 2.1–4 × 10<sup>3</sup>/cm<sup>2</sup>. The day after thawing and then every 2–3 days following, cells were refreshed with RPMI medium (Thermo Fisher Scientific, 21875034) supplemented with B27. Three days prior to patch clamp experiments, the medium was supplemented with 5% foetal calf serum. Patch clamp experiments were performed 7–10 days after initial cell seeding.

## Drug incubation

For chronic experiments, transfected HEK293A cells and SCN5A-1795insD hiPSC-CMs were incubated for 48 h in medium containing either vehicle (H<sub>2</sub>O) or mexiletine (Tocris Bioscience) at 37°C. HEK293A cells were then dissociated into single cells using trypsin (Thermo Fisher Scientific; final concentration 0.25%) for 2–3 min and re-suspended in medium without the drug (see scheme in Figures 1–6). Cells exhibiting green fluorescence were selected for electrophysiological experiments. Similarly, hiPSC-CMs incubated with mexiletine or vehicle were washed three times with RPMI/B27 medium supplemented with 5% serum prior to patch clamp experiments. To assess the acute effect of the drug, transfected HEK293A cells and SCN5A-1795insD hiPSC-CMs incubated for 48 h with mexiletine or vehicle were superfused for 5 min with 10 µM mexiletine (see scheme in Figures 2 and 4–6).

## Patch clamp analysis

### Data acquisition

Sodium current and APs were measured with the ruptured and perforated patch clamp technique, respectively, using an Axopatch 200B amplifier (Molecular Devices). Voltage control, data acquisition, and analysis were performed with pClamp10.6/Clampfit (Molecular Devices) and custom-made software for  $I_{Na}$  and APs, respectively. Borosilicate glass patch pipettes (Harvard Apparatus) with a tip resistance of 2–2.5 M $\Omega$  were used. Cell membrane capacitance was determined dividing the decay time constant of the capacitive transient in response to 5 mV hyperpolarizing steps from –40 mV, by the series resistance. Series resistance and cell membrane capacitance were compensated for  $\geq 80\%$ . Peak  $I_{Na}$  and APs were filtered at 5 kHz and digitized at 40 kHz, while late  $I_{Na}$  was filtered and digitized at 2 and 1 kHz, respectively. Peak  $I_{Na}$  was measured at room temperature, while late  $I_{Na}$  and APs were recorded at 37°C.

### Sodium current

Peak  $I_{Na}$  and late  $I_{Na}$  recordings in HEK293A cells were performed using a pipette solution containing the following (in mM): 110 CsF, 10 CsCl, 10 NaF, 1 MgCl<sub>2</sub>, 1 CaCl<sub>2</sub>, 2 Na<sub>2</sub>ATP, 11 EGTA, and 10 HEPES, pH 7.2 (CsOH). The bath solution contained the following (in mM): 140 NaCl, 10 CsCl, 2 CaCl<sub>2</sub>, 1 MgCl<sub>2</sub>, 5 glucose, and 10 HEPES, pH 7.4 (NaOH). In hiPSC-CMs, peak  $I_{Na}$  and late  $I_{Na}$  measurements were performed using the following external solution (in mM): 130 NaCl, 20 CsCl, 1.8 CaCl<sub>2</sub>, 1.2 MgCl<sub>2</sub>, 11 glucose, 0.005 nifedipine, and 5.0 HEPES, pH 7.4 (CsOH), and pipette solution containing (in mM) 3.0 NaCl, 133 CsCl, 2.0 MgCl<sub>2</sub>, 2.0 Na<sub>2</sub>ATP, 2.0 TEACl, 10.0 EGTA, and 5.0 HEPES, pH 7.3 (CsOH). Late  $I_{Na}$  was measured as 30 µM tetrodotoxin (TTX)-sensitive current, using a descending ramp protocol from a holding potential of –120 mV (cycle length of 5 s; see insets in Figures 3 and 4). In hiPSC-CMs, peak  $I_{Na}$  was elicited from a holding potential of –120 mV with a cycle length of 5 s, while in HEK293A cells, the holding potential was –140 mV (see insets in Figures 1, 2, and 6). Current–voltage ( $I$ – $V$ ) relationships and voltage dependency of activation were characterized with 500 ms depolarizing pulses between –100 and +60 mV (HEK293A cells) or +50 mV (hiPSC-CMs). Voltage dependency of inactivation was

analysed using a double-pulse protocol, with a 500 ms pre-pulse and a step to –20 mV. Sodium current was defined as the difference between peak and steady-state current at the end of each step. Current densities were calculated dividing the current amplitude by the cell membrane capacitance. Voltage dependence of activation and inactivation curves was fitted with Boltzmann function ( $y = [1 + \exp\{(V - V_{1/2})/k\}]^{-1}$ ), where  $V_{1/2}$  is the half-maximal voltage of (in)activation and  $k$  is the slope factor.

## Action potentials

Action potentials were measured using a modified Tyrode's solution containing the following (in mM): 140 NaCl, 5.4 KCl, 1.8 CaCl<sub>2</sub>, 1.0 MgCl<sub>2</sub>, 5.5 D-glucose, and 5 HEPES, pH 7.4 (NaOH). Pipettes were filled with the following (in mM): 125 K-gluconate, 20 KCl, 5 NaCl, 0.44 amphotericin B, and 10 HEPES, pH 7.2 (KOH). Action potentials were elicited at 1 Hz by 3 ms,  $\approx 1.2\times$  threshold current pulses through the patch pipette. To overcome the lack of the inward rectifying potassium current ( $I_{K1}$ ) in hiPSC-CMs, which limits the functional availability of  $I_{Na}$ ,<sup>23</sup> we injected a 2 pA/pF *in silico*  $I_{K1}$  with kinetics of Kir2.1 channels through dynamic clamp, as previously described and validated.<sup>24</sup> Resting membrane potential (RMP), AP amplitude (APA), maximal AP upstroke velocity ( $V_{max}$ ), and APD at 20, 50, and 90% repolarization (APD<sub>20</sub>, APD<sub>50</sub>, and APD<sub>90</sub>, respectively) were analysed. Data from 10 consecutive APs were averaged and potentials were corrected for the calculated liquid junction potential.<sup>25</sup>

## Statistical analysis

Data were analysed using Sigma Stat 3.5 (Systat Software Inc.) and GraphPad Prism version 8.4.3(686) for Windows (GraphPad Software). Values are shown as mean  $\pm$  SEM unless stated otherwise. Normality was tested by Kolmogorov–Smirnov. Unpaired Student's  $t$ -test, paired Student's  $t$ -test, Mann–Whitney test, and two-way RM ANOVA followed by Holm–Sidak test for *post hoc* analysis were used where appropriate and indicated in the relevant figures and tables. The level of statistical significance was set to  $P < 0.05$ .

## Results

### Chronic mexiletine incubation increases peak sodium current in SCN5A-WT and SCN5A-1795insD transfected HEK293A cells

We first assessed the chronic effect of mexiletine on WT  $I_{Na}$  and mutant  $I_{Na}$  using HEK293A cells transfected with either SCN5A-WT or SCN5A-1795insD. Cells were incubated with 10 µM mexiletine for 48 h followed by dissociation and resuspension in absence of the drug (see scheme in Figure 1A). SCN5A-1795insD cells showed a markedly reduced  $I_{Na}$  as compared to SCN5A-WT (Figure 1B–E), in line with the loss-of-function phenotype associated with the mutation. Chronic incubation with mexiletine resulted in a significant increase in average  $I_{Na}$  density in both SCN5A-WT (at –30 mV: 62.7%) and SCN5A-1795insD (at –30 mV: 93.6%) as compared to vehicle incubation (Figure 1B–E). Interestingly, the effect of mexiletine on peak  $I_{Na}$  appears larger on SCN5A-1795insD compared to SCN5A-WT, suggesting a possible preferential rescuing by mexiletine of mutant channels; however, further investigations are needed to confirm this. In Figure 1F and G and Supplementary material online, Table S1, the effects of 48 h mexiletine incubation on  $I_{Na}$  gating properties are depicted. While mexiletine did not impact on SCN5A-WT gating, it induced a significant shift towards more negative potentials for both voltage dependency of activation and inactivation in HEK293A cells transfected with SCN5A-1795insD. Mexiletine did not affect cell capacitance in either SCN5A-WT or in SCN5A-1795insD (data not shown). Overall, our findings indicate that chronic incubation with mexiletine at a clinically relevant dose of 10 µM is capable of increasing the presence of both SCN5A-WT and SCN5A-1795insD channels on the membrane.

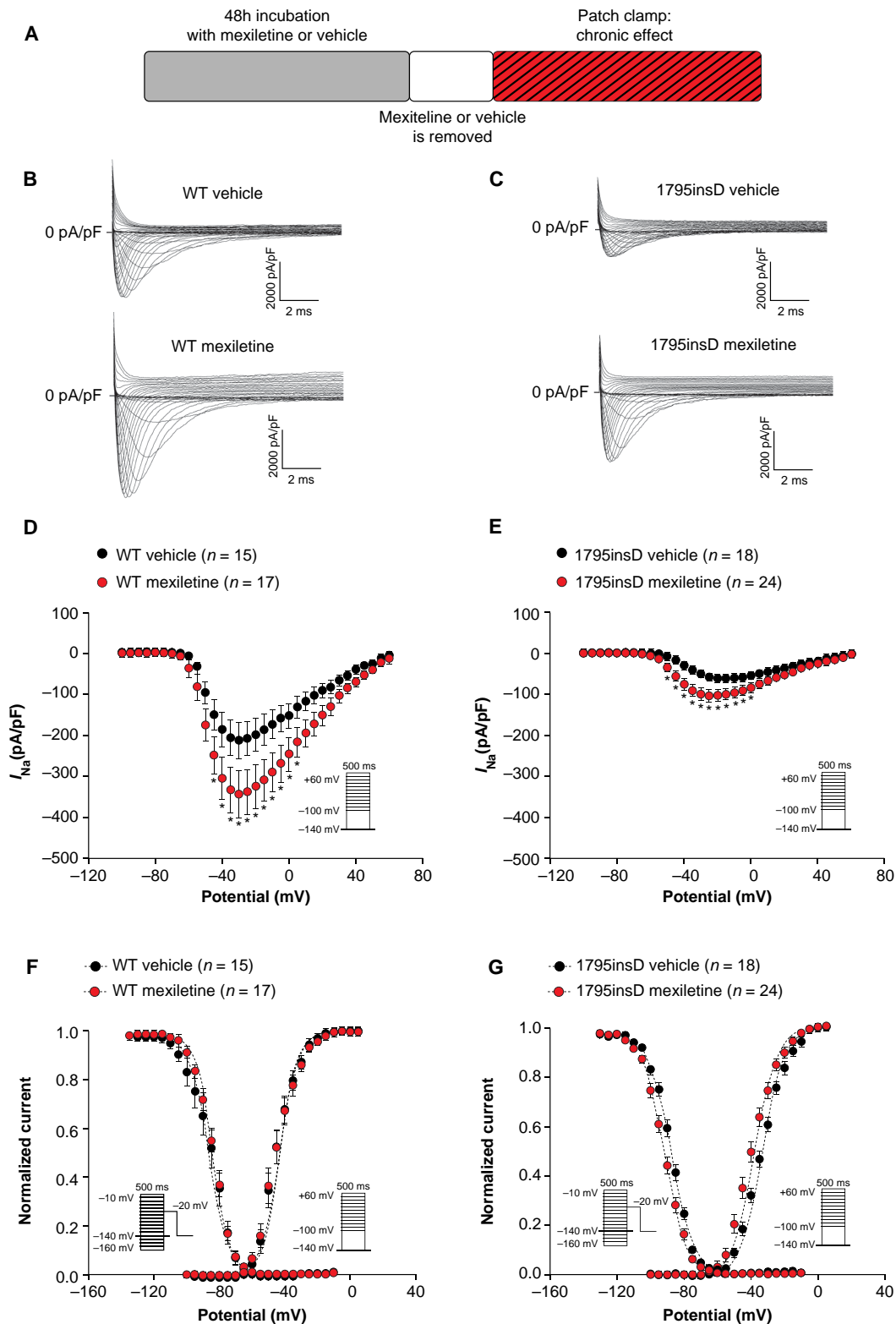


**Figure 1** Forty-eight hour incubation with  $10 \mu\text{M}$  mexiletine increases peak  $I_{\text{Na}}$  in HEK293A cells transfected with *SCN5A*-WT or *SCN5A*-1795insD. (A) Schematic representation of the performed experiments. (B, C) Representative  $I_{\text{Na}}$  traces recorded in HEK293A cells transfected with either *SCN5A*-WT (B) or *SCN5A*-1795insD (C) following 48 h incubation with vehicle or mexiletine ( $10 \mu\text{M}$ ). (D–G) Average peak  $I_{\text{Na}}$  current–voltage ( $I$ – $V$ ) relationships (D, E) and voltage dependence of activation and inactivation (F, G) in HEK293A cells transfected with *SCN5A*-WT or *SCN5A*-1795insD following 48 h incubation with vehicle or mexiletine ( $10 \mu\text{M}$ ). Insets: voltage protocols; \* $P < 0.05$ , two-way RM ANOVA followed by Holm–Sidak test for *post hoc* analysis. WT, wild-type.

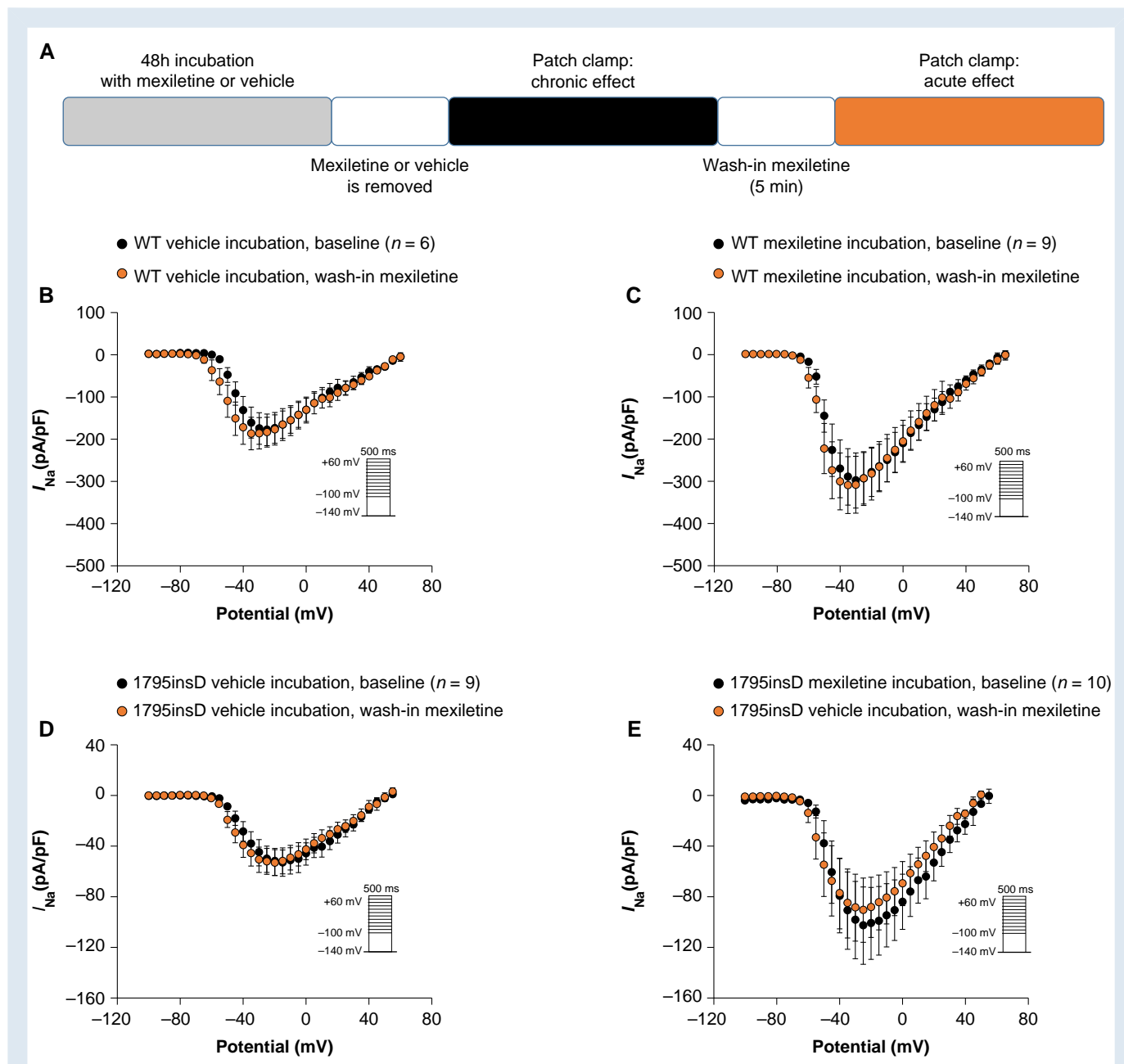


**Figure 2** Acute mexiletine treatment does not affect peak  $I_{Na}$  in HEK293A cells transfected with *SCN5A*-WT or *SCN5A*-1795insD previously incubated with either vehicle or mexiletine. (A) Schematic representation of the performed experiments. (B–E) Average peak  $I_{Na}$   $I$ - $V$  relationships before (baseline) and after 5 min wash-in of 10  $\mu$ M mexiletine in HEK293A cells transfected with *SCN5A*-WT (B, C) or *SCN5A*-1795insD (D, E), following 48 h incubation with either vehicle or mexiletine. WT, wild-type.

## Acute treatment with mexiletine does not affect peak sodium current in HEK293A cells transfected with either *SCN5A*-WT or *SCN5A*-1795insD

In the experiments presented in Figure 1, mexiletine was not present in the bath solution during patch clamp measurements in order to investigate specifically the chronic impact of the drug without its direct, acute effect on the channel. We next mimicked the clinical situation of chronic mexiletine therapy with continuous presence of the drug. For this purpose, we employed the same approach as in Figure 1A (48 h of

incubation with 10  $\mu$ M mexiletine or vehicle followed by dissociation and resuspension of cells in absence of the drug), but then acutely re-introduced mexiletine into the bath solution (10  $\mu$ M for 5 min) (see scheme in Figure 2A). Following chronic incubation with mexiletine or vehicle, acute treatment with mexiletine neither affected peak  $I_{Na}$  in HEK293A cells transfected with *SCN5A*-WT (Figure 2B and C) nor *SCN5A*-1795insD (Figure 2D and E). Hence, the beneficial increase of  $I_{Na}$  following 48 h mexiletine incubation was maintained upon acute (re-)application of mexiletine. Acute exposure to mexiletine did result in changes in voltage dependency of activation and inactivation for both *SCN5A*-WT and *SCN5A*-1795insD (data not shown). However, in a

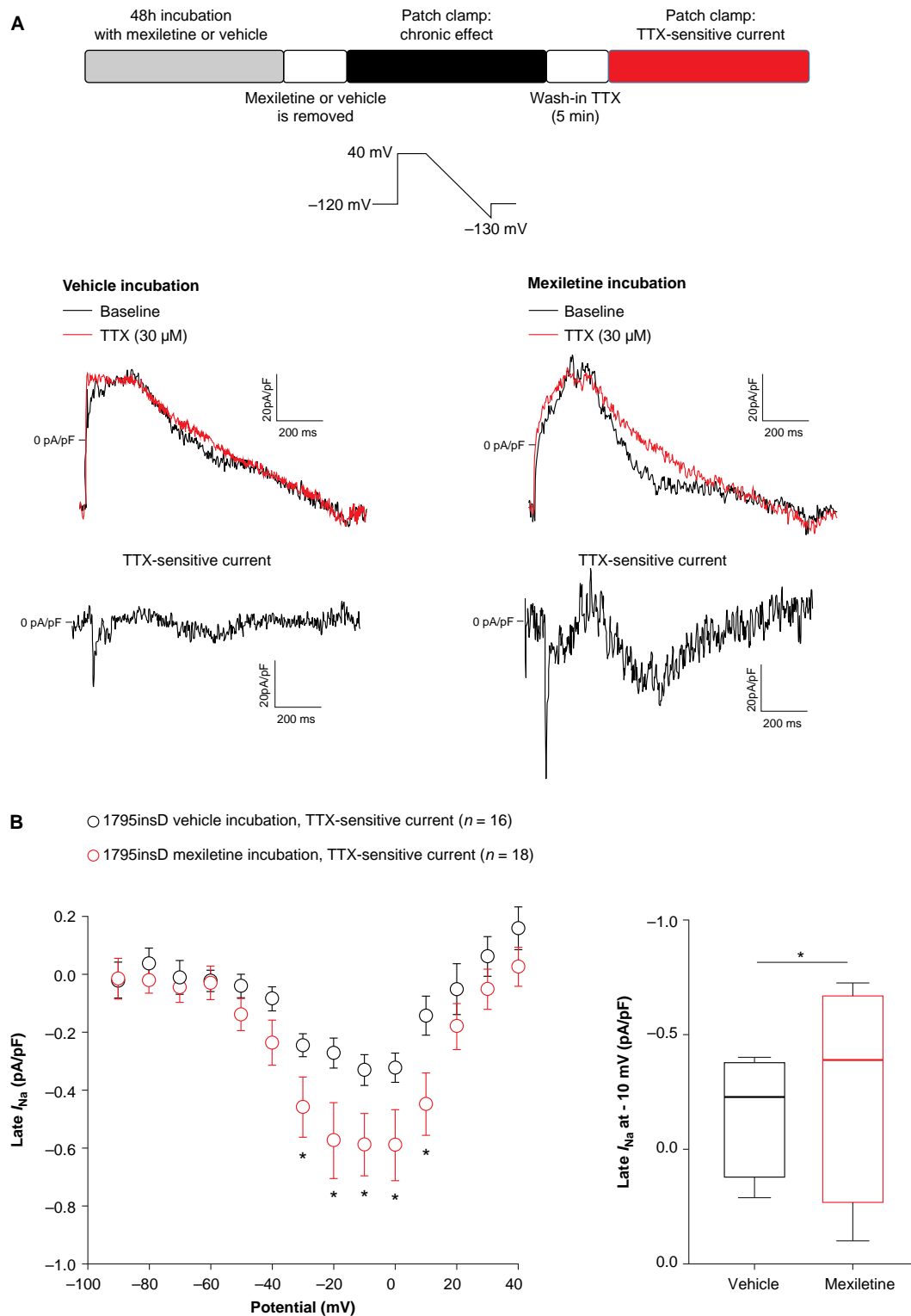


**Figure 3** Forty-eight hour incubation with mexiletine increases late  $I_{Na}$  in HEK293A cells transfected with *SCN5A-1795insD*. (A) Schematic representation of the performed experiments and typical late  $I_{Na}$  recordings obtained using a descending ramp protocol in HEK293A cells transfected with *SCN5A-1795insD* previously incubated for 48 h with vehicle (left panel) or mexiletine (right panel) before (baseline) and after application of 30  $\mu$ M TTX. TTX-sensitive current was obtained by subtraction of the current before and after application of TTX. (B) Average  $I$ - $V$  relationships for TTX-sensitive current in HEK293A cells transfected with *SCN5A-1795insD* previously incubated for 48 h with vehicle or mexiletine (left panel); \* $P < 0.05$ , two-way RM ANOVA followed by Holm-Sidak test for *post hoc* analysis. Boxplots (right panel) depicting late  $I_{Na}$  densities (median: boxes represent interquartile range; whiskers represent 95% interval) determined at -10 mV; \* $P < 0.05$ , Mann-Whitney test. TTX, tetrodotoxin.

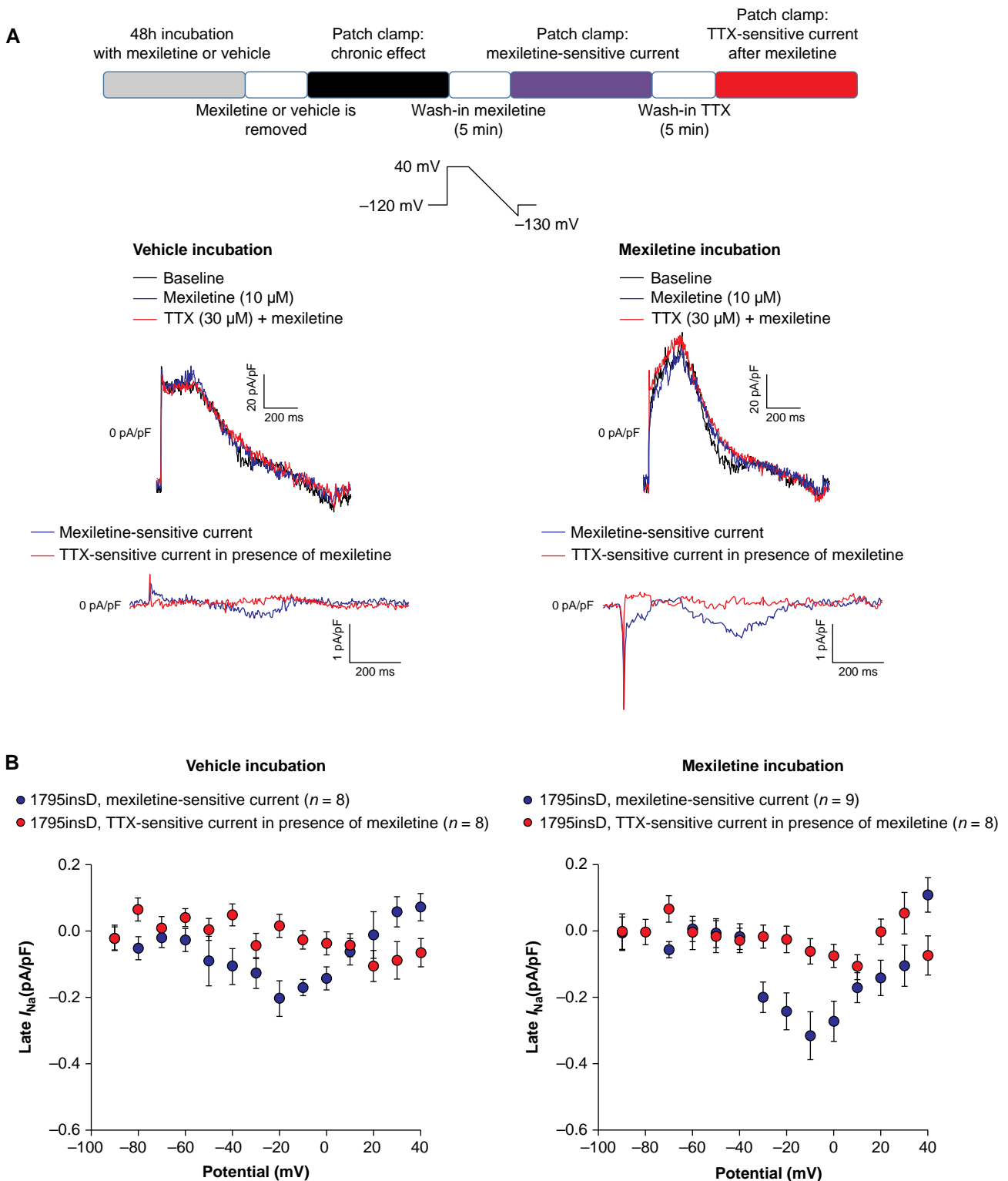


**Figure 4** Acute mexiletine treatment blocks late  $I_{Na}$  in HEK293A cells transfected with SCN5A-1795insD. (A) Schematic representation of the performed experiments (top panel). Typical late  $I_{Na}$  measurements obtained using a descending ramp protocol (see inset) in HEK293A cells transfected with SCN5A-1795insD previously incubated for 48 h with vehicle (middle left panel) and 10  $\mu$ M mexiletine (middle right panel) prior to drug application (baseline), after 5 min wash-in of mexiletine (10  $\mu$ M) and TTX (30  $\mu$ M) in the continued presence of mexiletine. The mexiletine-sensitive currents and TTX-sensitive currents in the presence of mexiletine are shown in the bottom panels. (B) Average  $I-V$  relationships for mexiletine-sensitive currents and TTX-sensitive current in the presence of mexiletine in HEK293A cells transfected with SCN5A-1795insD previously incubated for 48 h with vehicle (left panel) and mexiletine (right panel). The TTX-sensitive current in the presence of mexiletine is around the 0 pA/pF level, indicating that mexiletine already blocked completely late  $I_{Na}$ . TTX, tetrodotoxin.



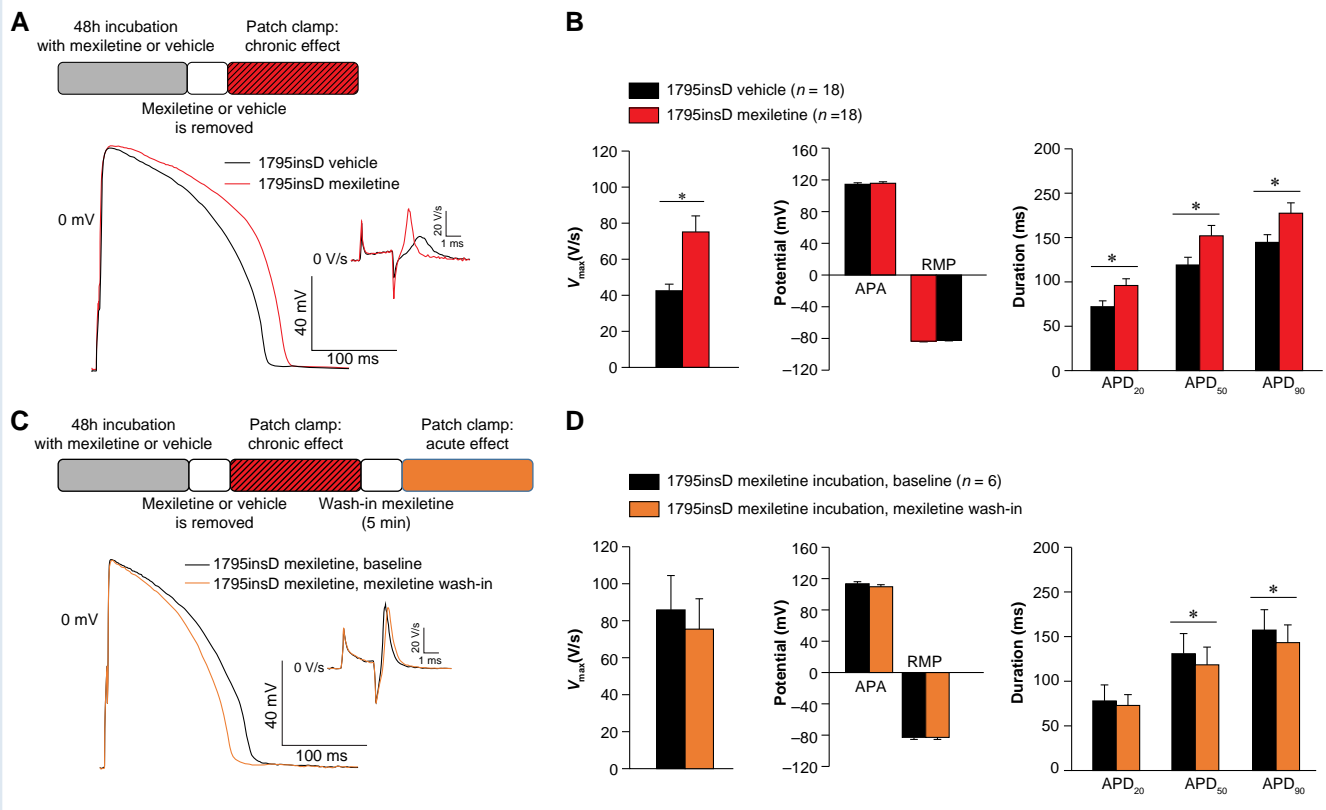


**Figure 5** Chronic and acute effects of mexiletine on action potential properties in SCN5A-1795insD hiPSC-CMs. (A) Schematic representation of the performed experiments and typical examples of APs recorded at 1 Hz in SCN5A-1795insD hiPSC-CMs after 48 h incubation with either vehicle or mexiletine (10  $\mu\text{M}$ ). (B) Average data for maximal upstroke velocity ( $V_{\text{max}}$ ), AP amplitude, resting membrane potential, AP duration at 20, 50, and 90% repolarization ( $\text{APD}_{20}$ ,  $\text{APD}_{50}$ , and  $\text{APD}_{90}$ ). \* $P < 0.05$ , unpaired Student's *t*-test. (C) Schematic representation of the performed experiments and typical examples of APs recorded at 1 Hz in SCN5A-1795insD hiPSC-CMs incubated for 48 h with mexiletine followed by removal of the drug (baseline) and after 5 min acute re-administration (wash-in) of mexiletine. (D) Average data for  $V_{\text{max}}$ , APA, RMP,  $\text{APD}_{20}$ ,  $\text{APD}_{50}$ , and  $\text{APD}_{90}$ . Insets: time derivatives of the AP upstrokes. \* $P < 0.05$ , paired Student's *t*-test. AP, action potential; APA, AP amplitude; RMP, resting membrane potential.

subset of cells where wash-out experiments were also performed, we were unable to reverse these effects of mexiletine, and a further negative shift of  $V_{1/2}$  of (in)activation was observed upon wash-out (see [Supplementary material online, Figures S1 and S2](#)). These results suggest a time-dependent effect rather than a direct effect of the drug on voltage dependence of (in)activation.

### Chronic effects of mexiletine on late sodium current in HEK293A cells transfected with SCN5A-1795insD

We next assessed the effect of chronic mexiletine incubation on late  $I_{\text{Na}}$  in HEK293A cells transfected with SCN5A-1795insD. To measure late  $I_{\text{Na}}$ , we used a descending ramp protocol that, in contrast to a single-step protocol, allows measurement of late  $I_{\text{Na}}$  across a dynamic voltage range simulating a plateau and repolarization phase of a cardiac AP.<sup>26</sup> Figure 3A shows typical examples of late  $I_{\text{Na}}$  recordings in cells chronically incubated either with vehicle (Figure 3A, left panel) or mexiletine (Figure 3A, right panel). Late  $I_{\text{Na}}$ , measured as TTX-sensitive current, was obtained by subtraction of the current recorded in the presence of 30  $\mu\text{M}$  TTX from the current recorded in the absence of the drug (baseline). Forty-eight hour incubation with mexiletine (followed by removal of the drug) significantly increased average late  $I_{\text{Na}}$  at  $-30$  to

+10 mV as compared to vehicle (Figure 3B, left panel). At  $-10$  mV, late  $I_{\text{Na}}$  was  $-0.33 \pm 0.05$  pA/pF ( $n = 16$ ) and  $-0.58 \pm 0.10$  pA/pF ( $n = 18$ ;  $P < 0.05$ , Mann-Whitney test) for vehicle and mexiletine, respectively (76.9% increase, Figure 3B, right panel).

### Acute effects of mexiletine on late sodium current in HEK293A cells transfected with SCN5A-1795insD

Following the observation that chronic mexiletine incubation increased late  $I_{\text{Na}}$  in HEK293A cells transfected with SCN5A-1795insD, we next investigated whether this could be mitigated by the acute effect of mexiletine. Late  $I_{\text{Na}}$  was measured in HEK293A cells transfected with SCN5A-1795insD previously incubated for 48 h with vehicle (Figure 4A, left panel) or mexiletine (Figure 4A, right panel), at baseline, after 5 min perfusion with mexiletine (10  $\mu\text{M}$ ), and after 5 min of TTX (see scheme in Figure 4A).

Mexiletine-sensitive current was obtained by subtraction of the current recorded in the presence of mexiletine from the baseline current, while TTX-sensitive current was measured by subtraction of the current recorded in the presence of TTX from the current measured after application of mexiletine. As shown in the typical examples in Figure 4A (middle panels), late  $I_{\text{Na}}$  is completely blocked by the acute application

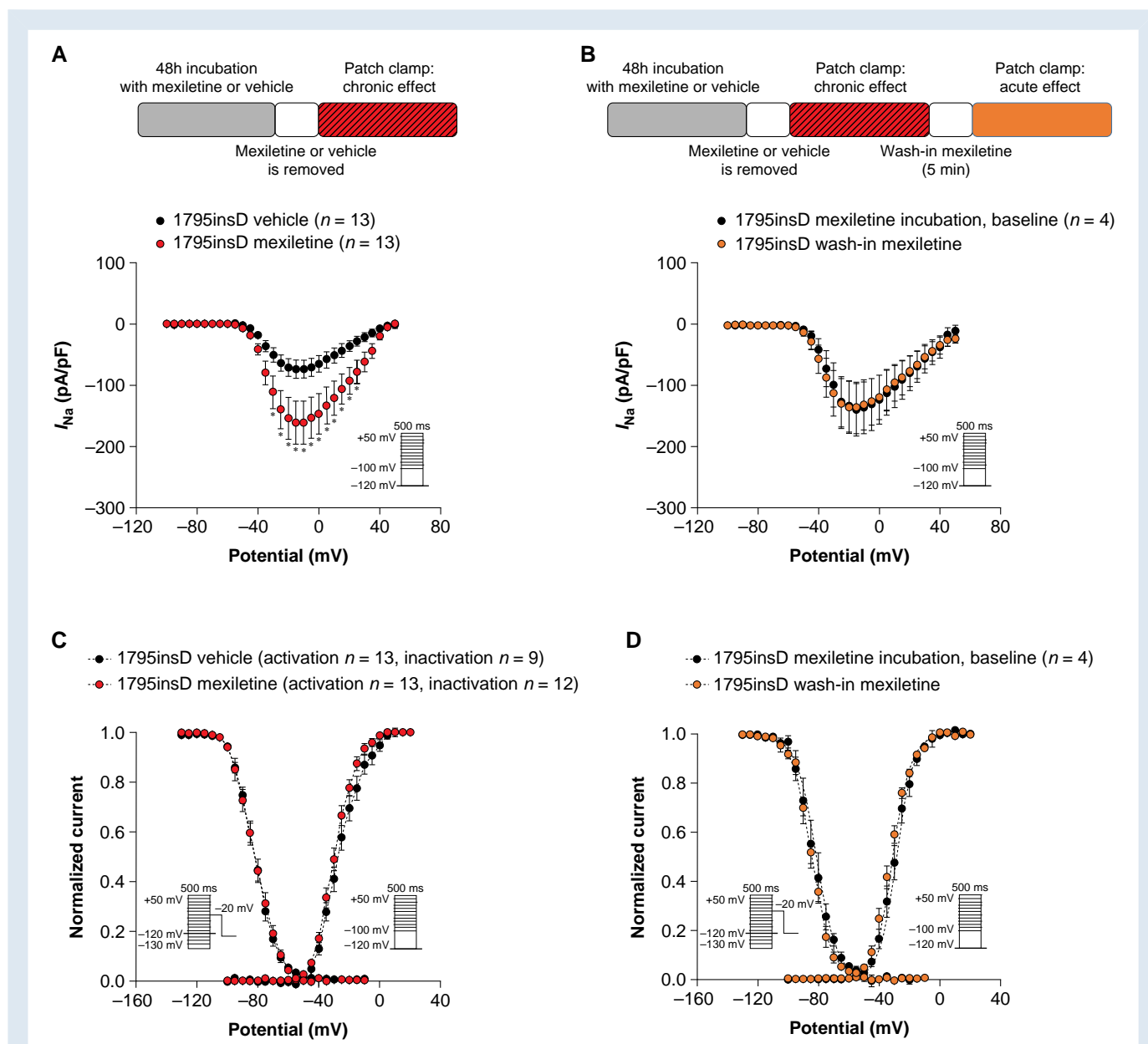


**Figure 6** Forty-eight hour incubation with  $10 \mu\text{M}$  mexiletine increases peak  $I_{Na}$  in SCN5A-1795insD hiPSC-CMs while acute mexiletine has no effect. (A, B) Schematic representations of the performed experiments (see panels) and average peak  $I_{Na}$   $I$ - $V$  relationships for SCN5A-1795insD hiPSC-CMs after 48 h incubation with vehicle or mexiletine ( $10 \mu\text{M}$ ) followed by removal of the drug (A) and after 5 min of re-administration (wash-in) of mexiletine ( $10 \mu\text{M}$ ) (B). (C, D) Voltage dependence of (in)activation measured in SCN5A-1795insD hiPSC-CMs after 48 h incubation with vehicle or mexiletine ( $10 \mu\text{M}$ ) followed by removal of the drug (C) and after 5 min re-administration (wash-in) of mexiletine (D). Insets: voltage protocols; \* $P < 0.05$ , two-way RM ANOVA followed by Holm-Sidak test for *post hoc* analysis.

of mexiletine in cells previously incubated chronically with either vehicle or mexiletine. Consequently, TTX-sensitive currents in acute presence of mexiletine are virtually absent (Figure 4A, bottom panels). This is further substantiated by the average  $I$ - $V$  relationships shown in Figure 4B.

Acute mexiletine treatment was able to block both the baseline mutation-induced late  $I_{Na}$  in vehicle-treated cells (at  $-10$  mV, chronic vehicle:  $-0.33 \pm 0.05$  pA/pF,  $n = 16$ , vs. after acute exposure to mexiletine:  $-0.03 \pm 0.03$  pA/pF,  $n = 8$ ) and the increased late  $I_{Na}$  induced by chronic exposure to mexiletine (at  $-10$  mV, chronic mexiletine:  $-0.58 \pm 0.10$  pA/pF,  $n = 18$ , vs. after acute exposure to mexiletine:  $-0.06 \pm 0.04$  pA/pF,  $n = 9$ ).

### Chronic mexiletine increases action potential upstroke velocity and peak sodium current in SCN5A-1795insD human-induced pluripotent stem cell-derived cardiomyocytes

To investigate the effect of mexiletine in a cardiomyocyte model that resembles more closely the heterozygote situation in patients, we performed experiments in hiPSC-CMs obtained from a SCN5A-1795insD patient.<sup>7</sup> We assessed the functional impact of mexiletine on AP

properties in *SCN5A*-1795insD hiPSC-CMs, employing dynamic clamp for *in silico*  $I_{K1}$  injection in cells paced at 1 Hz at physiological temperature. Incubation of hiPSC-CMs with mexiletine for 48 h, followed by removal of the drug, significantly increased  $V_{max}$  (76.6% increase) (Figure 5A and B and Supplementary material online, Table S2), thus importantly rescuing the loss-of-function part of this particular mutation. Acute re-administration of mexiletine following chronic exposure did not significantly affect  $V_{max}$  (Figure 5C and D and Supplementary material online, Table S3) and hence did not counteract the beneficial effects of chronic mexiletine on  $V_{max}$ . Action potential amplitude and RMP were not altered in response to chronic (Figure 5B and Supplementary material online, Table S2) or acute mexiletine treatment (Figure 5D and Supplementary material online, Table S3). Chronic administration of mexiletine for 48 h significantly increased APD<sub>20</sub>, APD<sub>50</sub>, and APD<sub>90</sub> in *SCN5A*-1795insD hiPSC-CMs (Figure 5A and B and Supplementary material online, Table S2), while acute re-administration of mexiletine significantly reduced APD<sub>50</sub> and APD<sub>90</sub> (Figure 5C and D and see Supplementary material online, Table S3). In line with the observed increase in  $V_{max}$ , 48 h incubation with mexiletine significantly increased  $I_{Na}$  density (at 15 mV: 119.2% increase; Figure 6A and Supplementary material online, Table S4) without any changes in voltage dependence of (in)activation (Figure 6C and Supplementary material online, Table S4); mexiletine also did not affect cell capacitance (data not shown). Acute re-administration of mexiletine following 48 h exposure to the drug affected neither  $I_{Na}$  density nor voltage dependence of (in)activation (Figure 6B and D and see Supplementary material online, Table S5), indicating that continued exposure to a therapeutic dose of mexiletine maintains the beneficial increase in peak  $I_{Na}$  induced by chronic mexiletine administration.

## Discussion

Given the complex mixed phenotype of both gain and loss of sodium channel function involved, *SCN5A* overlap syndromes may be difficult to treat.<sup>27–30</sup> We here assessed the beneficial effects of a clinically relevant concentration of mexiletine on the overlap mutation *SCN5A*-1795insD (associated with features of LQT3, BrS, and CCD, consequent to decreased peak  $I_{Na}$  and increased late  $I_{Na}$ ) and investigated for the first time its potential benefit in a human cardiomyocyte model. We first explored the effects of mexiletine in HEK293A cells, allowing us to assess its impact on *SCN5A*-WT vs. *SCN5A*-1795insD channels. By incubating HEK293A cells with mexiletine for 48 h followed by removal of the drug, we investigated specifically the chronic impact of mexiletine without its acute effect. Similar to what has previously been observed for other *SCN5A* mutations,<sup>14–18</sup> chronic mexiletine incubation of HEK293A cells transfected with *SCN5A*-1795insD increased peak  $I_{Na}$  and hence restored the loss-of-function phenotype. However, most previous studies employed high concentrations of mexiletine (>100  $\mu$ M),<sup>19–21</sup> which are far higher than the therapeutic concentration of 2.8–11  $\mu$ M, and are expected to decrease peak  $I_{Na}$  acutely. We observed chronically an increase in peak  $I_{Na}$  using a clinically relevant mexiletine concentration of 10  $\mu$ M; a similar effect was previously reported by Ruan et al., who demonstrated that 10  $\mu$ M mexiletine rescued the trafficking defect of the *SCN5A*-F1473S and restored peak  $I_{Na}$ .<sup>16</sup> Crucially, in our experiments, the acute re-administration of mexiletine at this concentration did not affect peak  $I_{Na}$  and thus did not counteract its chronic effect. In line with the apparent increase in membrane trafficking of *SCN5A*-1795insD channels, chronic incubation with mexiletine also resulted in a larger late  $I_{Na}$ . However, this detrimental effect was abrogated by the subsequent re-administration of mexiletine which blocked late  $I_{Na}$ , indicating its efficacious impact on the gain-of-function consequences of this mutation. Interestingly, chronic mexiletine incubation also significantly increased *SCN5A*-WT peak  $I_{Na}$ , which was again not abrogated by

acute re-administration of the compound. This indicates that mexiletine at a concentration of 10  $\mu$ M is also capable of enhancing membrane trafficking of WT  $Na_v1.5$ .

While the HEK293A cell data provided information on the distinct effects of mexiletine on *SCN5A*-WT vs. *SCN5A*-1795insD channels, this does not reflect the actual situation in patients who carry the mutation in heterozygous form. Moreover, HEK293A cells do not fully recapitulate the cardiomyocyte environment and lack many  $Na_v1.5$  interacting proteins.<sup>31</sup> We therefore also investigated the effect of mexiletine in hiPSC-CMs derived from a patient with the *SCN5A*-1795insD mutation, allowing us to assess its impact in a more clinically relevant model. Chronic incubation of *SCN5A*-1795insD hiPSC-CMs resulted in a robust increase in peak  $I_{Na}$  without impact on the gating properties. This indicates that the effects of mexiletine acted, as expected, by enhancing trafficking. In line with this increase in peak  $I_{Na}$ , chronic mexiletine also increased  $V_{max}$  and hence rescued the loss-of-function phenotype of the mutation. Acute re-administration of mexiletine following chronic incubation did not impact significantly on either peak  $I_{Na}$  or  $V_{max}$ , indicating that the concentration used was sufficiently high to promote trafficking of channels to the membrane, while not too high to cause an acute inhibition of peak  $I_{Na}$ . Chronic incubation of *SCN5A*-1795insD hiPSC-CMs with mexiletine also resulted in prolongation of APD<sub>20</sub>, APD<sub>50</sub>, and APD<sub>90</sub>. While this may reflect an increase in late  $I_{Na}$  as a result of enhanced trafficking of mutant channels (as observed in our HEK293A cell experiments), it may also be the consequence of mexiletine-mediated effects on other ion channels. In fact, acute mexiletine is known to also affect, at various concentrations, potassium channels such as hERG<sup>32,33</sup> and calcium channels.<sup>34–36</sup> Nevertheless, the fact that acute mexiletine reverted the prolongation of APD<sub>50</sub> and APD<sub>90</sub> induced by its chronic treatment is in line with a direct inhibiting effect of the drug on late  $I_{Na}$ . Since previous studies have shown a virtually undetectable late  $I_{Na}$  in HEK293 cells transfected with *SCN5A*-WT<sup>37</sup> and in control hiPSC-CMs,<sup>38,39</sup> we did not expect a measurable effect of mexiletine on late  $I_{Na}$  on WT channels or in control hiPSC-CMs and therefore did not investigate this.

The mechanism by which mexiletine acutely inhibits late  $I_{Na}$  is relatively well-established.  $Na_v1.5$  is formed by four domains (DI, DII, DIII, and DIV), each of which consists of six transmembrane segments (S1–S6), where S1–S4 helices include the voltage-sensing domains (VSD), S5 and S6 helices form the central pore domain, and DIII–DIV is the inactivation loop of the channel.<sup>40</sup> Mexiletine can bind two sites of  $Na_v1.5$  depending on the conformation of the channel: mexiletine-binding site 1, formed by the S6 segments from all four domains of the channel, and mexiletine-binding site 2 located within the fenestration between DIII and DIV.<sup>41</sup> The blocking effect of mexiletine on  $Na_v1.5$  is state-dependent<sup>42</sup> and concentration-dependent.<sup>43–46</sup> Mexiletine binds preferentially to the inactivated state of  $Na_v1.5$ , and consequently, *SCN5A* mutations that favour the inactivated state can facilitate mexiletine binding to  $Na_v1.5$ , thus resulting in a better clinical response to mexiletine treatment.<sup>13,16,47</sup> Previous studies have shown that mexiletine, at low concentration such as 10  $\mu$ M, inhibits preferentially late  $I_{Na}$  rather than peak  $I_{Na}$ ,<sup>43–46</sup> which is important to avoid pro-arrhythmic effects. How mexiletine increases the trafficking of  $Na_v1.5$  channels is not completely clear. It has been suggested that the drug acts as a ‘chemical chaperone’ by promoting correct protein folding and facilitating the exit of mutant ion channels trapped within the ER due to misfolding, allowing them to reach the membrane.<sup>15–17</sup> This same mechanism also has been suggested for chronic lidocaine treatment, another sodium channel blocker that is able to rescue sodium channel expression on the cell membrane.<sup>48</sup> Moreover, this concept of chemical rescue of impaired trafficking by drugs acting as chaperones has been demonstrated for other channels.<sup>49–51</sup> The molecular chaperone effect of mexiletine on  $Na_v1.5$  has been shown by immunofluorescence experiments<sup>15–17</sup> and more recently by surface

biotinylation assays in HEK293 cells.<sup>52</sup> Interestingly, in the latter study, the authors demonstrated that this trafficking rescuing effect is not universal but mutation-dependent. Moreover, when residues involved in mexiletine binding were mutated, mexiletine no longer impacted  $I_{Na,1.5}$  trafficking, demonstrating that the 'chaperone' effect of mexiletine requires its binding to the channel.<sup>52</sup>

Initially, *SCN5A*-1795insD patients appeared to be successfully managed by pacemaker therapy, aimed at preventing (nocturnal) bradycardia-dependent QT prolongation. However, ventricular arrhythmias and/or sudden cardiac death have recently been observed in a subset of patients despite pacemaker therapy.<sup>10</sup> Most of these patients were older than 40 years and were found to have hypertension as well as signs of cardiac hypertrophy, indicating potential differential age-dependent arrhythmia mechanisms. One may speculate that at later ages, the loss-of-function consequences of the mutation become more relevant for arrhythmogenesis. Indeed, development of cardiac fibrosis has been demonstrated in aged *Scn5a* haploinsufficient mice,<sup>53</sup> and a role for  $I_{Na,1.5}$  in modulating cardiac structure and function is increasingly recognized.<sup>54</sup> Hence, restoring the reduced  $I_{Na}$  is important to prevent conduction abnormalities, arrhythmias, and secondary cardiac remodelling. Our present observations that chronic mexiletine at a clinically relevant concentration rescues  $I_{Na}$  in *SCN5A*-1795insD hiPSC-CMs, without acutely affecting  $I_{Na}$ , demonstrate the first successful pharmacological approach to restore  $I_{Na}$ . However, it should be noted that mexiletine may also promote trafficking and plasma membrane localization of mutant channels and hence inadvertently increase late  $I_{Na}$  and repolarization disturbances, as occasionally observed clinically.<sup>55</sup> Given the fact that this effect on trafficking occurs only when used chronically, it will be essential to clinically monitor patients with (suspected) overlap syndrome mutations for such potential side effects, e.g. by performing ECG analysis 48 h after initiation of mexiletine treatment. Furthermore, our findings indicate that chronic administration of mexiletine can also increase *SCN5A*-WT peak  $I_{Na}$ , raising the intriguing possibility that it may also prove efficacious in (inherited) conditions associated with reduced  $I_{Na}$  aside from *SCN5A* channelopathy, including BrS and arrhythmogenic cardiomyopathy.

In conclusion, here we demonstrate for the first time the therapeutic benefit of a clinically relevant dose of mexiletine in a human cardiomyocyte model of *SCN5A* overlap syndrome. Furthermore, we identified mexiletine as a novel approach to rescue decreased peak  $I_{Na}$ , which may prove beneficial in other inherited arrhythmia disorders.

## Supplementary material

Supplementary material is available at *Europace* online.

## Acknowledgements

We thank M.P.H. Mol for technical assistance in culturing the hiPSC and Tiziana Errera for statistical support.

## Funding

This study was supported by the Netherlands CardioVascular Research Initiative (CVON-PREDICT2 2018-30 and CVON-eDETECT 2015-12), Fondation Leducq (17CVD02), a ZonMw Priority Medicines (PMRare) grant (113303006), a ZonMw PSIDER grant (10250042110010), and a Novo Nordisk Foundation grant (NNF21CC0073729).

**Conflict of interest:** None declared

## Data availability

All relevant data are within the manuscript and its online supplementary material.

## Translational perspective

The sodium channel blocker mexiletine may reduce the enhanced late sodium current secondary to gain-of-function *SCN5A* mutations and consequently have beneficial effects in long QT syndrome type 3. In addition, high concentrations of mexiletine have been shown to rescue peak sodium current for certain loss-of-function mutations, most likely by restoring trafficking of mutant channels. Here, we demonstrate that a clinically relevant concentration of mexiletine has a dual beneficial effect in a human cardiomyocyte model of *SCN5A* overlap syndrome. Our findings furthermore identify mexiletine as a therapeutic approach to rescue decreased peak sodium current, with potential benefit for other inherited arrhythmia disorders.

## References

- Nerbonne JM, Kass RS. Molecular physiology of cardiac repolarization. *Physiol Rev* 2005; **85**:1205–53.
- O'Reilly M, Sommerfeld LC, O'Shea C, Broadway-Stringer S, Andaleeb S, Reyat JS et al. Familial atrial fibrillation mutation M1875T-*SCN5A* increases early sodium current and dampens the effect of flecainide. *Europace* 2023; **25**:1152–61.
- Calloe K, Geryk M, Freude K, Treat JA, Vold VA, Frederiksen HRS et al. The G213D variant in *Nav1.5* alters sodium current and causes an arrhythmogenic phenotype resulting in a multifocal ectopic Purkinje-related premature contraction phenotype in human-induced pluripotent stem cell-derived cardiomyocytes. *Europace* 2022; **24**: 2015–27.
- Remme CA, Bezzina CR. Sodium channel (dys)function and cardiac arrhythmias. *Cardiovasc Ther* 2010; **28**:287–94.
- Bezzina C, Veldkamp MW, van den Berg MP, Postma AV, Rook MB, Viersma J-W et al. A single  $Na^{+}$  channel mutation causing both long-QT and Brugada syndromes. *Circ Res* 1999; **85**:1206–13.
- Remme CA, Verkerk AO, Nuyens D, van Ginneken ACG, van Brunschot S, Belterman CNW et al. Overlap syndrome of cardiac sodium channel disease in mice carrying the equivalent mutation of human *SCN5A*-1795insD. *Circulation* 2006; **114**:2584–94.
- Davis RP, Casini S, van den Berg CW, Hoekstra M, Remme CA, Dambrot C et al. Cardiomyocytes derived from pluripotent stem cells recapitulate electrophysiological characteristics of an overlap syndrome of cardiac sodium channel disease. *Circulation* 2012; **125**:3079–91.
- Moss AJ, Zareba W, Hall WJ, Schwartz PJ, Crampton RS, Benhorin J et al. Effectiveness and limitations of beta-blocker therapy in congenital long-QT syndrome. *Circulation* 2000; **101**:616–23.
- Priori SG, Napolitano C, Schwartz PJ, Grillo M, Bloise R, Ronchetti E et al. Association of long QT syndrome loci and cardiac events among patients treated with beta-blockers. *Jama-J Am Med Assoc* 2004; **292**:1341–4.
- Rivaud MR, Jansen JA, Postema PG, Nannenber EA, Mizusawa Y, van der Nagel R et al. A common co-morbidity modulates disease expression and treatment efficacy in inherited cardiac sodium channelopathy. *Eur Heart J* 2018; **39**:2898–907.
- van der Ree MH, van Dussen L, Rosenberg N, Stolwijk N, van den Berg S, van der Wel V et al. Effectiveness and safety of mexiletine in patients at risk for (recurrent) ventricular arrhythmias: a systematic review. *Europace* 2022; **24**:1809–23.
- Farkowski MM, Karlinski M, Pytkowski M, de Asmundis C, Lewandowski M, Mugnai G et al. Mexiletine for recurrent ventricular tachycardia in adult patients with structural heart disease and implantable cardioverter defibrillator: an EHRA systematic review. *Europace* 2022; **24**:1504–11.
- Moreno JD, Zhu W, Mangold K, Chung W, Silva JR. A molecularly detailed  $Na(V)1.5$  model reveals a new class I antiarrhythmic target. *JACC Basic Transl Sci* 2019; **4**:736–51.
- Valdivia CR, Ackerman MJ, Tester DJ, Wada T, McCormack J, Ye B et al. A novel *SCN5A* arrhythmia mutation, M1766L, with expression defect rescued by mexiletine. *Cardiovasc Res* 2002; **55**:279–89.
- Valdivia CR, Tester DJ, Rok BA, Porter CBJ, Munger TM, Jahangir A et al. A trafficking defective, Brugada syndrome-causing *SCN5A* mutation rescued by drugs. *Cardiovasc Res* 2004; **62**:53–62.
- Ruan Y, Denegri M, Liu N, Bachetti T, Seregni M, Morotti S et al. Trafficking defects and gating abnormalities of a novel *SCN5A* mutation question gene-specific therapy in long QT syndrome type 3. *Circ Res* 2010; **106**:1374–83.
- Moreau A, Keller D, Huang H, Fressart V, Schmied C, Timour Q et al. Mexiletine differentially restores the trafficking defects caused by two Brugada syndrome mutations. *Front Pharmacol* 2012; **3**:62.
- Hu R-M, Tester DJ, Li R, Sun T, Peterson BZ, Ackerman MJ et al. Mexiletine rescues a mixed biophysical phenotype of the cardiac sodium channel arising from the *SCN5A* mutation, N406K, found in LQT3 patients. *Channels (Austin)* 2018; **12**:176–86.
- Monk JP, Brogden RN. Mexiletine. A review of its pharmacodynamic and pharmacokinetic properties, and therapeutic use in the treatment of arrhythmias. *Drugs* 1990; **40**: 374–411.

20. Takahashi MP, Cannon SC. Mexiletine block of disease-associated mutations in S6 segments of the human skeletal muscle Na<sup>+</sup> channel. *J Physiol* 2001;**537**:701–14.
21. Wang GK, Russell C, Wang SY. Mexiletine block of wild-type and inactivation-deficient human skeletal muscle hNav1.4 Na<sup>+</sup> channels. *J Physiol* 2004;**554**:621–33.
22. van den Brink L, Brandao KO, Yiangou L, Mol MPH, Grandela C, Mummery CL et al. Cryopreservation of human pluripotent stem cell-derived cardiomyocytes is not detrimental to their molecular and functional properties. *Stem Cell Res* 2020;**43**:101698.
23. Verkerk AO, Wilders R. Dynamic clamp in electrophysiological studies on stem cell-derived cardiomyocytes—why and how? *J Cardiovasc Pharm* 2021;**77**:267–79.
24. van Putten RM, Mengarelli I, Guan K, Zegers JG, van Ginneken AC, Verkerk AO et al. Ion channelopathies in human induced pluripotent stem cell derived cardiomyocytes: a dynamic clamp study with virtual IK1. *Front Physiol* 2015;**6**:7.
25. Barry PH, Lynch JW. Liquid junction potentials and small cell effects in patch-clamp analysis. *J Membr Biol* 1991;**121**:101–17.
26. Casini S, Marchal GA, Kawasaki M, Nariswari FA, Portero V, van den Berg NWE et al. Absence of functional Na(v)1.8 channels in non-diseased atrial and ventricular cardiomyocytes. *Cardiovasc Ther* 2019;**33**:649–60.
27. Schwartz PJ, Priori SG, Locati EH, Napolitano C, Cantu F, Towbin JA et al. Long QT syndrome patients with mutations of the SCN5A and HERG genes have differential responses to Na<sup>+</sup> channel blockade and to increases in heart rate. Implications for gene-specific therapy. *Circulation* 1995;**92**:3381–6.
28. Shimizu W, Antzelevitch C. Sodium channel block with mexiletine is effective in reducing dispersion of repolarization and preventing torsade des pointes in LQT2 and LQT3 models of the long-QT syndrome. *Circulation* 1997;**96**:2038–47.
29. Wang HW, Zheng YQ, Yang ZF, Li CZ, Liu YM. Effect of mexiletine on long QT syndrome model. *Acta Pharmacol Sin* 2003;**24**:316–20.
30. Mazzanti A, Maragna R, Faragli A, Monteforte N, Bloise R, Memmi M et al. Gene-specific therapy with mexiletine reduces arrhythmic events in patients with long QT syndrome type 3. *J Am Coll Cardiol* 2016;**67**:1053–8.
31. Selga E, Sendfeld F, Martinez-Moreno R, Medine CN, Tura-Ceide O, Wilmot SI et al. Sodium channel current loss of function in induced pluripotent stem cell-derived cardiomyocytes from a Brugada syndrome patient. *J Mol Cell Cardiol* 2018;**114**:10–9.
32. Gualdani R, Tadini-Buoninsegni F, Roselli M, Defrenza I, Contino M, Colabufo NA et al. Inhibition of hERG potassium channel by the antiarrhythmic agent mexiletine and its metabolite m-hydroxymexiletine. *Pharmacol Res Perspect* 2015;**3**:e00160.
33. Johnson M, Gomez-Galeno J, Ryan D, Okolotowicz K, McKeithan WL, Sampson KJ et al. Human iPSC-derived cardiomyocytes and pyridyl-phenyl mexiletine analogs. *Bioorg Med Chem Lett* 2021;**46**:128162.
34. Abbate E, Boulakia M, Coudiere Y, Gerbeau JF, Zitoun P, Zemzemi N. In silico assessment of the effects of various compounds in MEA/hPSC-CM assays: modeling and numerical simulations. *J Pharmacol Toxicol Methods* 2018;**89**:59–72.
35. Yonemizu S, Masuda K, Kurata Y, Notsu T, Higashi Y, Fukumura K et al. Inhibitory effects of class I antiarrhythmic agents on Na<sup>+</sup> and Ca<sup>2+</sup> currents of human iPSC cell-derived cardiomyocytes. *Regen Ther* 2019;**10**:104–11.
36. Ono K, Kiyosue T, Arita M. Comparison of the inhibitory effects of mexiletine and lidocaine on the calcium current of single ventricular cells. *Life Sci* 1986;**39**:1465–70.
37. Casini S, Tan HL, Bhuiyan ZA, Bezzina CR, Barnett P, Cerbai E et al. Characterization of a novel SCN5A mutation associated with Brugada syndrome reveals involvement of D11S4–S5 linker in slow inactivation. *Cardiovasc Res* 2007;**76**:418–29.
38. Terrenoire C, Wang K, Tung KW, Chung WK, Pass RH, Lu JT et al. Induced pluripotent stem cells used to reveal drug actions in a long QT syndrome family with complex genetics. *J Gen Physiol* 2013;**141**:61–72.
39. Portero V, Casini S, Hoekstra M, Verkerk AO, Mengarelli I, Belardinelli L et al. Anti-arrhythmic potential of the late sodium current inhibitor GS-458967 in murine Scn5a-1798insD<sup>+</sup>/– and human SCN5A-1795insD<sup>+</sup>/– iPSC-derived cardiomyocytes. *Cardiovasc Res* 2017;**113**:829–38.
40. DeMarco KR, Clancy CE. Cardiac Na channels: structure to function. *Curr Top Membr* 2016;**78**:287–311.
41. Li G, Voltz RL, Wang CY, Ren L, He PX, Yu SD et al. Gating properties of mutant sodium channels and responses to sodium current inhibitors predict mexiletine-sensitive mutations of long QT syndrome 3. *Front Pharmacol* 2020;**11**:1182.
42. Nakagawa H, Munakata T, Sunami A. Mexiletine block of voltage-gated sodium channels: isoform- and state-dependent drug-pore interactions. *Mol Pharmacol* 2019;**95**:236–44.
43. Wang DW, Yazawa K, Makita N, George AL, Jr., Bennett PB. Pharmacological targeting of long QT mutant sodium channels. *J Clin Invest* 1997;**99**: 1714–20.
44. Zhu W, Mazzanti A, Voelker TL, Hou P, Moreno JD, Angsutararux P et al. Predicting patient response to the antiarrhythmic mexiletine based on genetic variation. *Circ Res* 2019;**124**:539–52.
45. Kim HJ, Kim BG, Park JE, Ki CS, Huh J, Youm JB et al. Characterization of a novel LQT3 variant with a selective efficacy of mexiletine treatment. *Sci Rep* 2019;**9**:12997.
46. Rotordam MG, Obergrussberger A, Brinkwirth N, Takasuna K, Becker N, Horváth A et al. Reliable identification of cardiac conduction abnormalities in drug discovery using automated patch clamp II: best practices for Nav1.5 peak current in a high throughput screening environment. *J Pharmacol Toxicol Methods* 2021;**112**:107125.
47. Desaphy JF, De Luca A, Tortorella P, De Vito D, George AL Jr, Conte Camerino D. Gating of myotonic Na channel mutants defines the response to mexiletine and a potent derivative. *Neurology* 2001;**57**: 1849–57.
48. Zhao J, Ziane R, Chatelier A, O’Leary ME, Chahine M. Lidocaine promotes the trafficking and functional expression of Na(v)1.8 sodium channels in mammalian cells. *J Neurophysiol* 2007;**98**:467–77.
49. Martin GM, Chen PC, Devaraneni P, Shyng SL. Pharmacological rescue of trafficking-impaired ATP-sensitive potassium channels. *Front Physiol* 2013;**4**:386.
50. Guo J, Zhang X, Hu Z, Zhuang Z, Zhu Z, Chen Z et al. A422t mutation in HERG potassium channel retained in ER is rescuable by pharmacologic or molecular chaperones. *Biochem Biophys Res Commun* 2012;**422**:305–10.
51. Martin GM, Sung MW, Shyng SL. Pharmacological chaperones of ATP-sensitive potassium channels: mechanistic insight from cryoEM structures. *Mol Cell Endocrinol* 2020;**502**:110667.
52. Gando I, Campana C, Tan RB, Cecchin F, Sobie EA, Coetzee WA. A distinct molecular mechanism by which phenytoin rescues a novel long QT 3 variant. *J Mol Cell Cardiol* 2020;**144**:1–11.
53. Royer A, van Veen TA, Le Bouter S, Marionneau C, Griol-Charhbil V, Leoni AL et al. Mouse model of SCN5A-linked hereditary Lenegre’s disease: age-related conduction slowing and myocardial fibrosis. *Circulation* 2005;**111**:1738–46.
54. Rivaud MR, Delmar M, Remme CA. Heritable arrhythmia syndromes associated with abnormal cardiac sodium channel function: ionic and non-ionic mechanisms. *Cardiovasc Res* 2020;**116**:1557–70.
55. Calloe K, Schmitt N, Grubb S, Pfeiffer R, David JP, Kanter R et al. Multiple arrhythmic syndromes in a newborn, owing to a novel mutation in SCN5A. *Can J Physiol Pharmacol* 2011;**89**:723–36.